SPARC-BD-04/002
25 October 2004

Studies of Gaussian Pulse Shaping at SPARC

M.Boscolo, M.Ferrario *(INFN-LNF)*, S. Reiche *(UCLA Dept. Of Physics/Astronomy)*

Abstract

The SPARC nominal working point is optimized for a flat top pulse with rise time of 1ps. In this paper we discuss the implications of a Gaussian longitudinal pulse. Complete start-to-end simulations are presented for the proposed working point. Advantages and drawbacks of the Gaussian and flat pulse shapes are discussed. It is shown that the two cases provide the same saturation length and average power, but the higher current in the beam core of the Gaussian pulse gives a higher peak radiation power. As the laser pulse shape could be Gaussian at the first stage of the operation, it is clear the importance of these simulation results.

Presented at the SPARC Collaboration Workshop Frascati, 25-27 October 2004

1 INTRODUCTION

The starting point of our simulation studies has been a longitudinal Gaussian charge distribution. Start-to-end simulations have been performed for different parameters sets. Results have been compared to the SPARC nominal working point [1]. The nominal pulse is square with L=10 ps and a rise time of 1ps.

The simulation study aimed at understanding the behaviour of a Gaussian beam for our injector/FEL system. For this reason different dimensions of the Gaussian have been considered. All the free parameters have been varied, to understand how the matching conditions change due to the different space-charge force. In section 3 PARMELA simulations are discussed in detail, showing how the optimization of the free parameters has been carried on.

The most promising results have been obtained with a Gaussian of σ=2.89 ps and with all the other parameters equal to the nominal values but for a reduction of the injection phase by some degrees.

For this selected working point the FEL simulations predict saturation along the undulator. Complete GENESIS simulations are presented in section 4.

2 GAUSSIAN BEAM

The first assumption has been to take a Gaussian with the same σ_{rms} of the nominal square pulse of L=10 ps, so that to preserve the matching conditions with the beam line. The σ_{rms} of a square pulse is given by $L/\sqrt{12}$ so a Gaussian of σ=2.89 ps is taken. The two beam initial profiles are shown in fig. 1. This assumption implies that the Gaussian beam has a 40% higher current. In fact:

$$I_{Square} = \frac{\lambda c Q}{\pi R^2 L} \quad ; \quad I_{Gaussian} = \frac{\lambda c Q}{\pi R^2 \sqrt{2\pi}\sigma_z} e^{-z^2/2\sigma_z^2}$$

so that for the central slice:

$$I_G = \sqrt{\frac{6}{\pi}} I_S \cong 1.4 I_S .$$

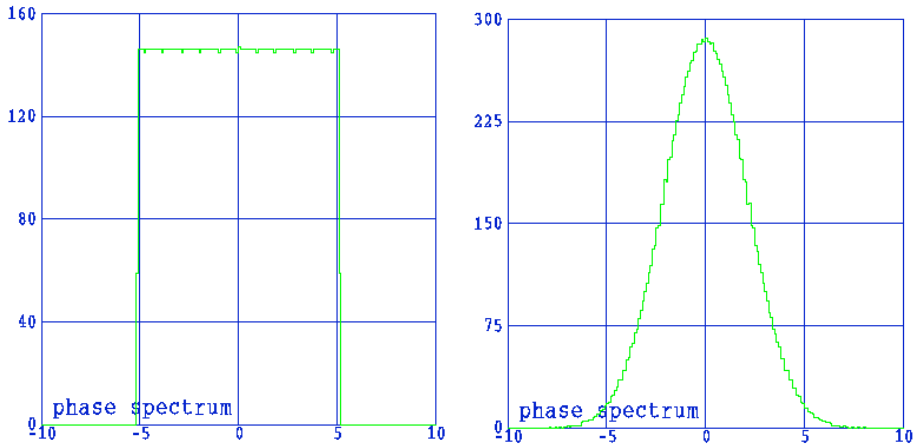

FIG. 1: Beam profiles with the same σ_{rms} :(left) square pulse with L=10ps; (right) Gaussian pulse with σ=2.89 ps.

In fig. 2 is the emittance and beam envelope evolution along the first 2 m of the injector

without traveling waves for a Gaussian pulse (red line) compared to a square pulse (black line) and to a square pulse with 1 ps of rise time (blue line). The comparison shows that for the Gaussian pulse the first emittance minimum almost disappears, as also pointed out in [2].

We know from that for a square pulse with high rise time it is expected a similar behavior, as shown in fig. 3, taken from [3].

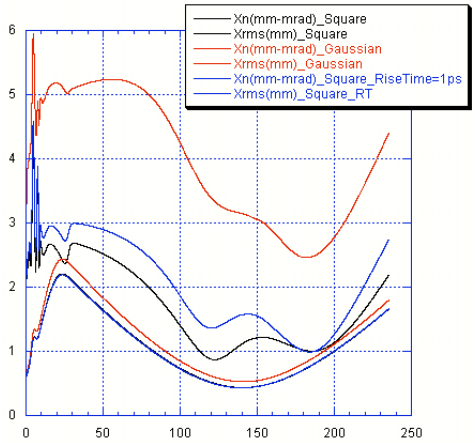

FIG. 2: Beam emittance and envelope along the SPARC injector without travelling waves for a square pulse (black line), for a square pulse with 1ps of rise time (blue line) and for a Gaussian pulse of □=2.89ps (red line).

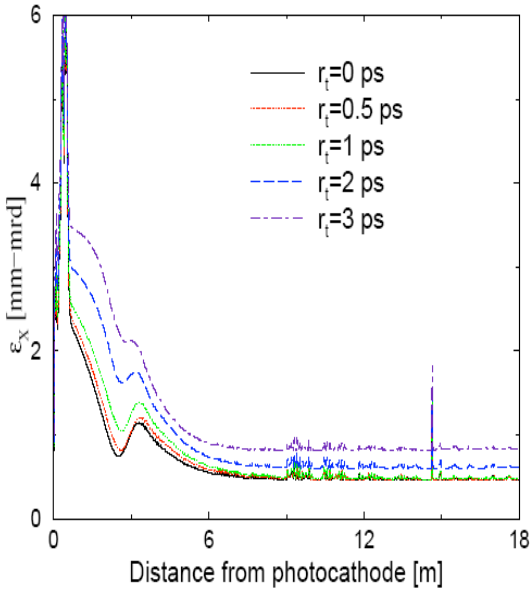

FIG. 3: Sensitivity of the transverse emittance to the rise time of the laser r_t (from [3]).

In fig. 3 is the sensitivity of the transverse emittance for different rise times of the laser pulse. It is shown in the plot that at the increase of the rise time the first emittance minimum decreases until it disappears.

In this sense we can say that a Gaussian pulse behaves like square pulse with high rise time.

In fig.4 emittance and rms beam size are plotted for different Gaussian □, and with all the other parameters constant.

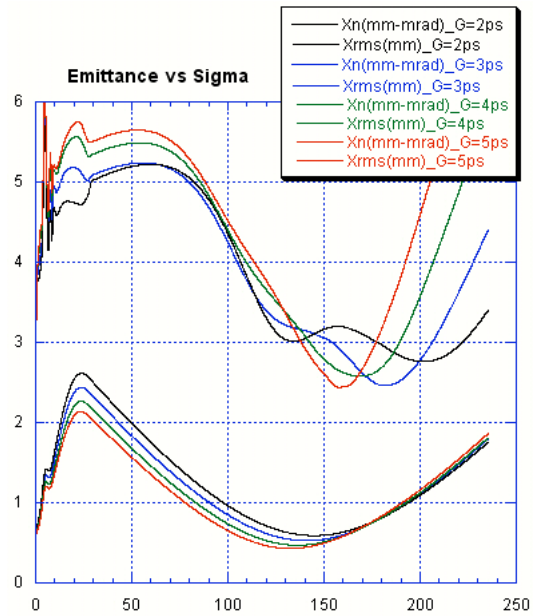

FIG. 4: Beam emittance and envelope for different □ of the Gaussian profile.

3 PARMELA SIMULATIONS

The Gaussian electron beam pulse is propagated through the SPARC photoinjector, which has a configuration of parameters fixed by the flat-top pulse optimization transport. The idea was to investigate the Gaussian beam characteristics which could be best transported along the accelerator. Moreover, for a given Gaussian beam, we have tried to optimize the matching conditions varying the free parameters, which are the magnetic value of the gun solenoid B(gun) and the injection phase □(inj). The other two parameters which can be varied to optimize the working point for the Gaussian pulse are the transverse spot radius R and the temporal pulse length. In fact, by slightly moving them from the nominal values, it is possible in principle to adjust the space-charge force to optimize the matching conditions.

The goal is to find a set of parameters for the Gaussian pulse such that the emittance evolution along z without travelling waves has two relative emittance minima, and the minimum of the beam envelope should correspond to the relative maximum. In this way we would have matched the Gaussian beam to the beam line.

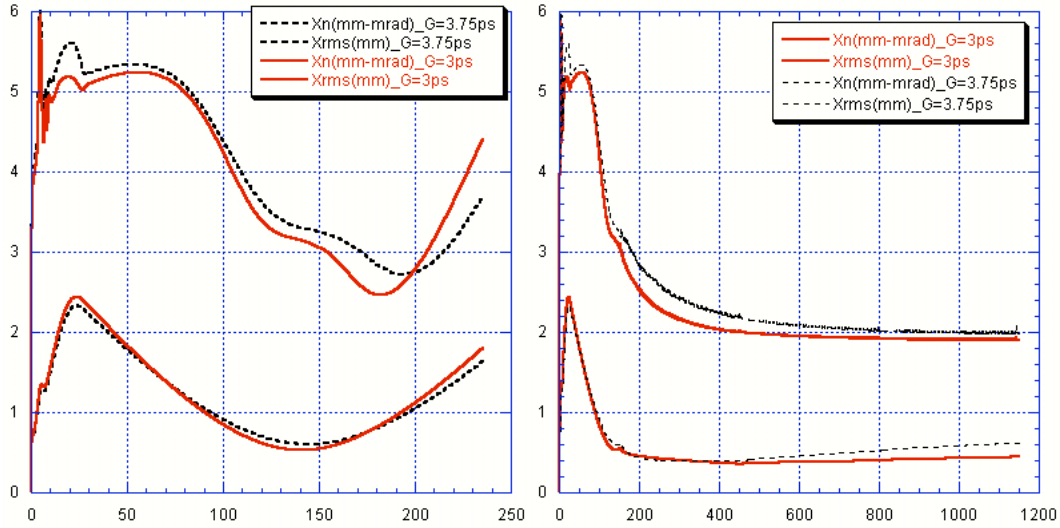

FIG. 5: Beam emittance and envelope without *(left plot)*.and with *(right plot)* TW. Full red line is for case 1: □=2.89 ps; B(gun)=2.73KG; □(inj)=28°; dotted black line is for case 2: □=3.75ps; B(gun)=2.70KG; □(inj)=26°.

Different working points with good emittance and energy spread have been found. In particular, we have selected the two cases, see fig. 5:

1. □=2.89 ps; Q=1.1nC; R=1.13mm; B(gun)=2.73KG; □(inj)=28°; B(ITW)=0.1KG
2. □=3.75ps; Q=1.1nC; R=1.13mm; B(gun)=2.70KG; □(inj)=26°; B(ITW)=0.1KG

These two working points have the same projected emittance at the transfer line entrance, of about $\varepsilon_{x,rms} \approx 2\pi m$ and the same energy spread. In the following, we discuss the working point for the Gaussian pulse of □=2.89 ps (case 1) which provides a higher peak current in the central slices, and we compare it to the nominal square pulse case.

In fig.6 and fig.7 the rms and the slice parameter values are shown, respectively. Left and right plots are referred to the Gaussian and to the square pulse, respectively.

The rms energy spread is ~0.13% for the Gaussian and ~0.16% for the square pulse (lower left plots in fig.6 a and b). As for the emittance, the projected value given by the Gaussian working point is 1.9 □m, which is a high value if compared to the flat top case 0.7 □m (see upper plots of fig.6 a and b).

The slice emittance is about ~1 □m for all the central slices of the beam obtained by a Gaussian pulse (lower plots of fig.7a). This value is higher than the nominal case shown in the lower plots of fig.5b where most slices have an emittance of ~0.5 □m. It is discussed in section 4 that the slice values for the Gaussian case are however good enough to give good performances for the SASE/FEL process.

These simulations are promising essentially for the high current in the beam core of the Gaussian, as shown in the upper right plot of fig.7 a. In table 1 is the beam current per slice. The current distribution along the bunch reproduces the Gaussian shape, the central slices have current as high as ~130-140 A. For the square pulse case (see upper right plot of fig.7 b) the current distribution is more flat along the bunch, and the peak current for the central slices is ~110 A.

TAB. 1: Beam current slice values for the Gaussian pulse case 1.

slice	Slice Current [A]
1	9.3
2	41.6
3	73.6
4	101.6
5	120.2
6	133.7
7	141.7
8	141.3
9	132.5
10	114.1
11	86.4
12	49.9
13	11.7

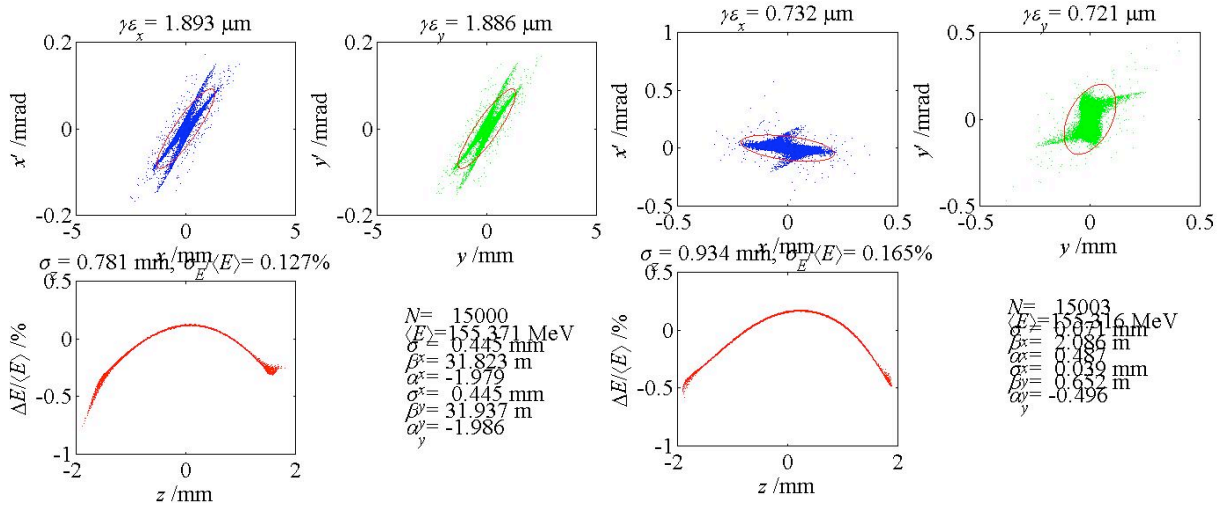

(a) ***(b)***

FIG. 6: ***(a)*** Rms parameter values for case 1. □=2.89 ps; ***(b)*** Rms parameter values for flat top pulse L=10ps and rise time=1ps at the undulator entrance. *Upper left plot*: projected horizontal emittance; *upper right plot*: projected vertical emittance; *lower left plot*: energy spread.

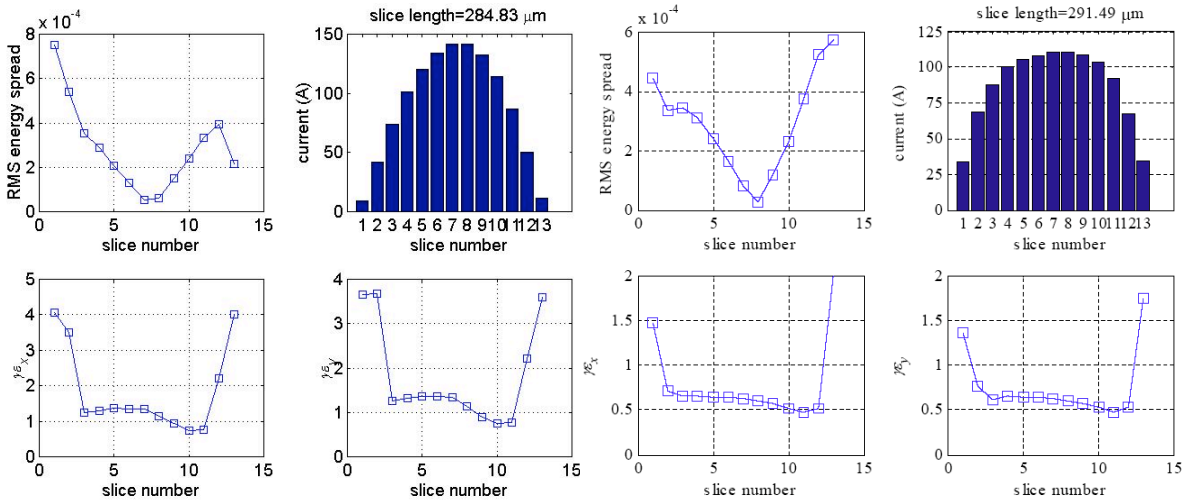

(a) *(b)*

FIG. 7: ***(a)*** Slice analysis for case 1. □=2.89 ps; ***(b)*** Slice analysis for flat top pulse L=10ps and rise time=1ps at the undulator entrance. *Upper left plot*: projected slice rms energy spread; *upper right plot*: slice current; *lower left plot*: slice radial emittance; *lower right plot*: slice vertical emittance.

4 SASE FEL PERFORMANCE WITH GAUSSIAN PULSE SHAPE

FEL/SASE simulations performed with the code GENESIS are presented here. They are referred to the Gaussian pulse shape discussed in the previous section, and the predictions are compared to the nominal square pulse case.

In fig.8 is the average power radiated by the electron beam as it passes through the undulator. The left plot is relative to the Gaussian pulse, the right plot to the nominal one. It appears that average power is equal for the two cases. Moreover, in both cases saturation at 10 m from the undulator entrance is expected.

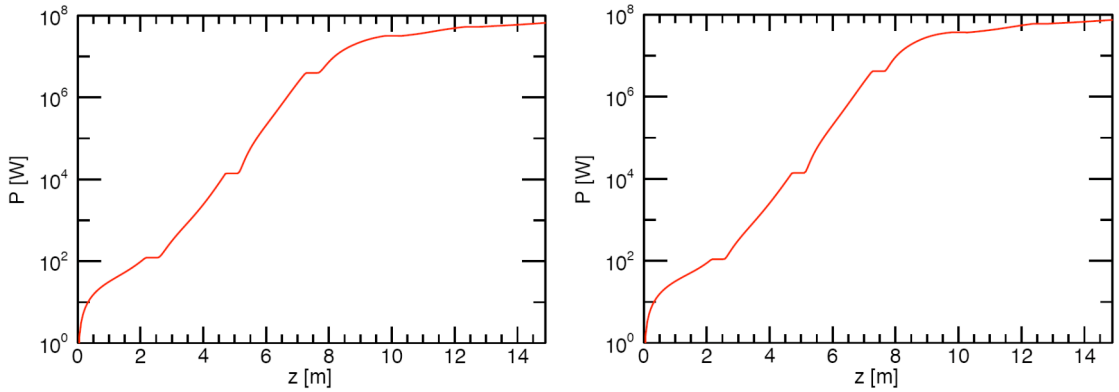

FIG. 8: Average power radiated by the electron beam through the undulator **for the** ***(left plot)*** Gaussian profile; ***(right plot)*** flat profile.

On the other hand, due to the different pulse shape at the undulator entrance, the peak power is different for the two cases. The Gaussian pulse has a current higher by 40% with respect to the flat profile, this induces to a different peak radiation power. The radiation pulse is shorter because not all the slices are good enough to drive the SASE instability and has

higher spikes than that of the flat profile (see fig. 9). The photon flux is greater for the flat profile, where about ~75-80% of the beam is lasing, to be compared to about ~65% of the Gaussian beam.

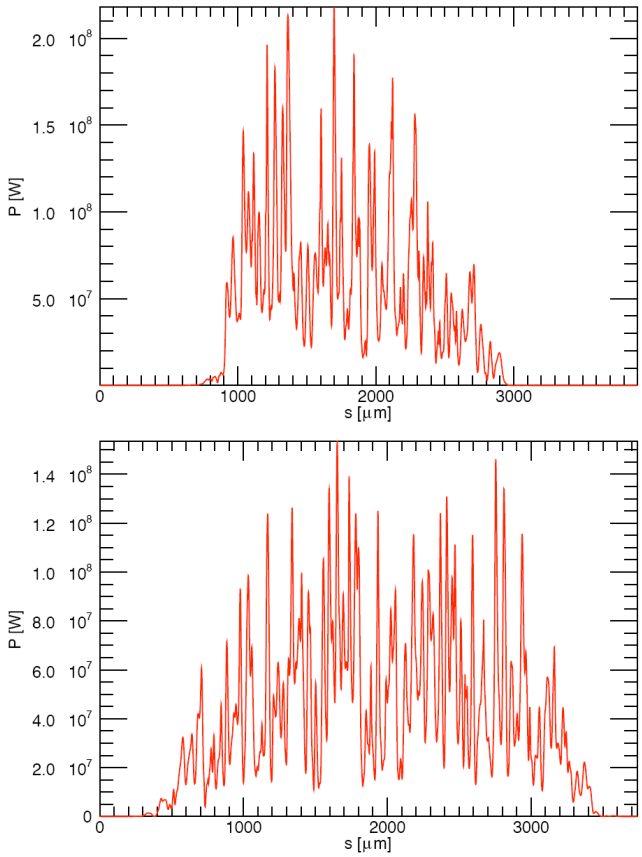

FIG. 9: ***(upper plot)*** Gaussian profile; ***(lower plot)*** flat profile of radiated power at 10m of the undulator.

5 GAUSSIAN WITH LOWER CURRENT

In this last section we shortly discuss the case of a Gaussian with lower current. The parameter values have been rescaled to keep the beam volume constant, so with a charge of Q=0.6 nC the spot radius results R=0.924 mm with a sigma of □=2.36 ps.

The idea is to investigate the case of a beam core with a current of approximately I~100A and with low current tails. In this way only the central slices of the beam should undergo the FEL/SASE process. In fig.10 is plotted the emittance and envelope evolution along the beamline. Projected emittance is now $\varepsilon_{x,rms} \approx 1.3 \mu m$ with an rms energy spread of ~0.085% (see lower left plot of fig.11).

In this case the average radiated power (see fig. 12) is lower than the previous cases, as expected. In any case, saturation is reached at 10 m.

In fig. 13 the radiation pulse and spectrum are shown, at saturation.

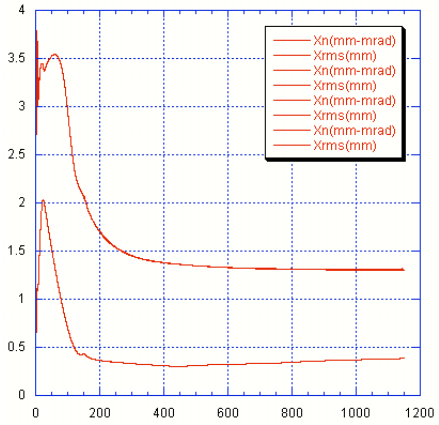

FIG. 10: Gaussian of Q=0.6nC; R=0.924mm and □=2.36 ps: beam emittance and envelope.

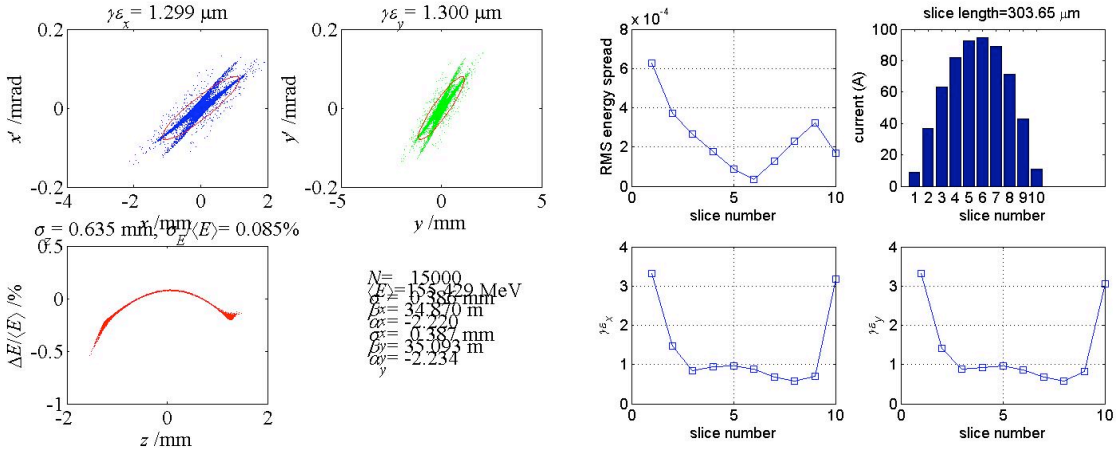

FIG. 11: Gaussian of Q=0.6nC; R=0.924mm and □=2.36 ps: ***(left plot)*** rms parameter values; ***(right plot)*** slice analysis.

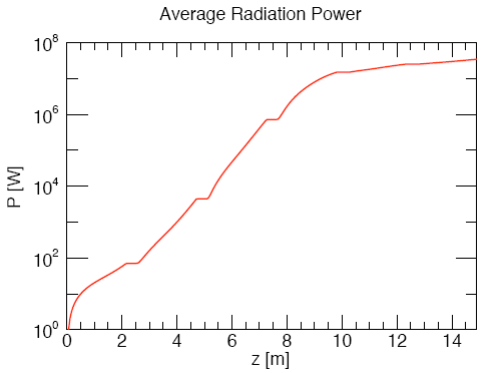

FIG. 12: Average power radiated by the electron beam through the undulator.

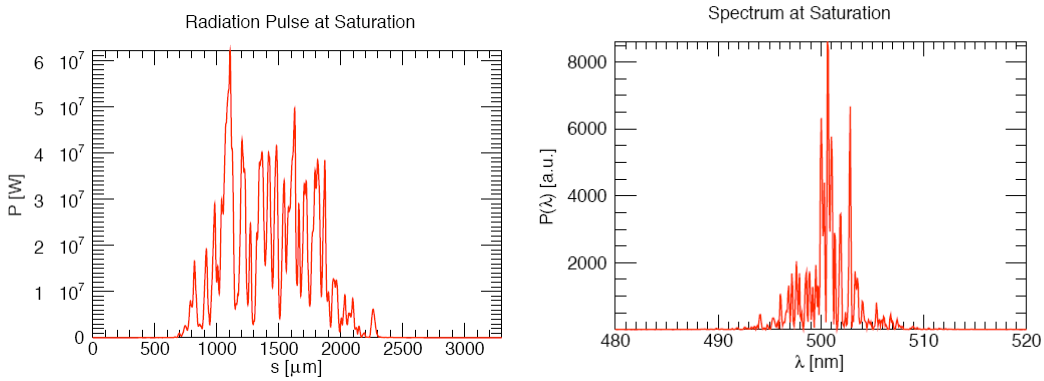

FIG. 13: ***(left plot)*** radiated power at saturation; ***(right plot)*** spectrum of radiation emitted at saturation.

6 CONCLUSIONS

In the first stage of the SPARC commissioning it is possible that the laser pulse will not be the square nominal pulse. We have investigated the consequences of a Gaussian pulse, optimizing a working point for the best Gaussian that can be transported along the beam line.

Complete start-to-end simulations predict the same saturation length and average power, but a shorter radiation pulse with a higher peak power than the square case.

7 REFERENCES

[1] D.Alesini et al, “Status of the SPARC Project” EPAC04, Lucerne (2004).
[2] Yujong Kim, “ Experiment Based TTF2 Injector Simulation” TESLA_S2E_2004_35, July 27, 2004
[3] M. Ferrario, K. Floettmann, B. Grigoryan, t. Limberg, Ph. Piot, “Conceptual Design of the TESLA XFEL Photoinjector”, TESLA-FEL 2001-3